Comparative transcriptome analysis between long- and short-term survival after pig-to-monkey cardiac xenotransplantation reveals differential heart failure development

Byeonghwi Lim, Min-Jae Jang, Seung-Mi Oh, Jin Gu No, Jungjae Lee, Sang Eun Kim, Sun A. Ock, Ik Jin Yun, Junseok Kim, Hyun Keun Chee, Wan Seop Kim, Hee Jung Kang, Kahee Cho, Keon Bong Oh & Jun-Mo Kim

View supplementary material

Published online: 04 Oct 2023.

Submit your article to this journal

Article views: 175

View related articles

View Crossmark data

Taylor & Francis
Taylor & Francis Group

🔓 OPEN ACCESS | Check for updates

Comparative transcriptome analysis between long- and short-term survival after pig-to-monkey cardiac xenotransplantation reveals differential heart failure development

Byeonghwi Lim [a], Min-Jae Jang [a], Seung-Mi Oh [a], Jin Gu No [b], Jungjae Lee [a], Sang Eun Kim [b], Sun A. Ock [b], Ik Jin Yun [c], Junseok Kim [d], Hyun Keun Chee [d], Wan Seop Kim [e], Hee Jung Kang [f], Kahee Cho [g], Keon Bong Oh [b] and Jun-Mo Kim [a]

aDepartment of Animal Science and Technology, Chung-Ang University, Anseong, Republic of Korea; bAnimal Biotechnology Division, National Institute of Animal Science, RDA, Wanju, Republic of Korea; cDepartments of Surgery, Konkuk University Medical Center, Konkuk University School of Medicine, Seoul, Republic of Korea; dDepartments of Thoracic and Cardiovascular Surgery, Konkuk University Medical Center, Konkuk University School of Medicine, Seoul, Republic of Korea; eDepartments of Pathology, Konkuk University Medical Center, Konkuk University School of Medicine, Seoul, Republic of Korea; fDepartment of Laboratory Medicine, Hallym University College of Medicine, Hallym University Sacred Heart Hospital, Anyang, Republic of Korea; gPrimate Organ Transplantation Centre, Genia Inc., Seongnam, Republic of Korea

ABSTRACT

Cardiac xenotransplantation is the potential treatment for end-stage heart failure, but the allogenic organ supply needs to catch up to clinical demand. Therefore, genetically-modified porcine heart xenotransplantation could be a potential alternative. So far, pig-to-monkey heart xenografts have been studied using multi-transgenic pigs, indicating various survival periods. However, functional mechanisms based on survival period-related gene expression are unclear. This study aimed to identify the differential mechanisms between pig-to-monkey post-xenotransplantation long- and short-term survivals. Heterotopic abdominal transplantation was performed using a donor CD46-expressing GTKO pig and a recipient cynomolgus monkey. RNA-seq was performed using samples from POD60 XH from monkey and NH from age-matched pigs, D35 and D95. Gene-annotated DEGs for POD60 XH were compared with those for POD9 XH (Park et al. 2021). DEGs were identified by comparing gene expression levels in POD60 XH versus either D35 or D95 NH. 1,804 and 1,655 DEGs were identified in POD60 XH versus D35 NH and POD60 XH versus D95 NH, respectively. Overlapped 1,148 DEGs were annotated and compared with 1,348 DEGs for POD9 XH. Transcriptomic features for heart failure and inhibition of T cell activation were observed in both long (POD60)- and short (POD9)-term survived monkeys. Only short-term survived monkey showed heart remodeling and regeneration features, while long-term survived monkey indicated multi-organ failure by neural and hormonal signaling as well as suppression of B cell activation. Our results reveal differential heart failure development and survival at the transcriptome level and suggest candidate genes for specific signals to control adverse cardiac xenotransplantation effects.

Introduction

Heart transplantation is the only treatment for end-stage heart failure, but the clinical supply of allogenic organ is greatly scarce (Lund et al. 2017; Rossano et al. 2017; Längin et al. 2018). Cardiac xenotransplantation can be a potential alternative (Cooper and Pierson 2022; Kobashigawa 2022). Currently, pigs are considered the most appropriate donors, because they are similar to humans in size and physiology, and have a large litter size and a short maturation period (Cooper et al. 2002). To date, pig-to-monkey heart xenografts have been widely studied using various wild-type and transgenic pigs and monkeys, including baboon, cynomolgus, and rhesus (Cooper et al. 2014; Lee et al. 2018), but solving immunological rejections and dysregulations remain a challenge (Lu et al. 2020).

Heart xenograft usually causes three main rejections: hyperacute rejection (HAR), acute humoral xenograft

rejection (AHXR), and acute cellular rejection (Cascalho and Platt 2001; Lu et al. 2020). HAR and AHXR were nearly removed by using α-1,3-galactosyltransferase gene-knockout (GTKO) pigs expressing human complement regulatory proteins such as CD46, CD55, and CD59, in addition to exogenous immunosuppressive therapies (Mohiuddin et al. 2014, 2016). However, coagulation dysregulation is another barrier (Cooper et al. 2016), resulting in thrombotic microangiopathy (TM), systemic consumptive coagulopathy (CC), and systemic inflammatory response (Bühler et al. 2000; Cooper and Bottino 2015; Long et al. 2016). To prevent coagulation problems, various combinatorial expressions of human coagulation regulation proteins such as thrombomodulin and CD39, and anti-inflammatory protein, CD73, in pigs have been utilized (Fischer et al. 2016; Mohiuddin et al. 2016; Lee et al. 2018). Although these techniques were used to tackle coagulation dysregulation, survival periods were still irregular even with the same immunosuppressive therapies, especially in cynomolgus monkeys (Lee et al. 2018). Therefore, comparing gene expression patterns between long- and short-term survival periods in xenotransplanted hearts may help understand what determines the survival of cynomolgus monkeys transplanted with hearts from transgenic pigs. RNA-seq is one of useful methods for understanding biological mechanisms (Ahn et al. 2022; Kim et al. 2022).

In this study, we detected changes in transcriptomes based on RNA-seq data between the xenotransplanted heart (XH) of postoperative day 60 (POD60) monkey and normal heart (NH) of age-matched pigs, and performed comparative analyses between XHs of POD60 and POD9 monkeys to understand survival period-related differences.

Materials and methods

Ethics statement

The experimental procedures were approved by the Orient Bio Institutional Animal Care and Use Committee (IACUC No. ORIENT-IACUC-16141 and ORIENT-IACUC-19015). All procedures conformed to the guidelines from the NIH Guide for the Care and Use of Laboratory Animals.

Animals and surgery

A 35-day-old (D35) male homozygous GTKO pig expressing human CD46 was used as a donor. Pre-transplantation porcine heart weight was 35.00 g. The recipient, a five-year-old male cynomolgus monkey (*Macaca fascicularis*), was housed in a clean cage. The body weight of

the monkey on the day of transplantation was 6.27 kg. Surgery was performed using heterotopic abdominal method (Yang et al. 2017), and immunosuppression was also induced in the monkey. Details are described in Supplementary materials.

Euthanasia

Before euthanasia, anesthesia was induced with an intravenous bolus of ketamine 30 mg/kg and xylazine 3 mg/kg. The monkey at terminal was sacrificed by inducing exsanguination from vena cava and abdominal artery under anesthesia.

Xenotransplanted porcine cardiac tissue collection

Small fragments collected randomly with ventricle samples were plunged into liquid nitrogen for RNA-seq or 4% paraformaldehyde for histological analyses. An age-matched litter of the donor (D35 GTKO) and age-matched litter of the POD60 (D95 GTKO) were sacrificed, and their NH samples were collected. Figure 1(A) shows a schematic overview of this study.

Hematological and biochemical analysis of a cynomolgus monkey

The recipient blood parameters were analyzed on POD −7, 0, 3, 8, 14, 21, 28, 35, 42, 49, 57 and 60. Detailed methods are described in a previous study (Park et al. 2021). Comparative analysis was performed using hematological parameters of short-term survived (POD9 XH) monkey.

Histological analysis

The specimens were immobilized in 10% neutral buffered formalin and embedded in paraffin. The paraffin blocks were sliced to a thickness of 3 μm. The sections were deparaffinized, rehydrated, and stained with hematoxylin and eosin.

RNA-Seq

Total RNA was isolated from NH (D35 and D95 pigs) and XH POD60 tissues using TRIzol method. To check the quality of extracted RNA, RNA-integrity number (RIN) was calculated using 2100 Bioanalyzer (Table S1). Total cDNA was synthesized for library construction. Constructed libraries were analyzed with Illumina HiSeq 4000 (Illumina, Inc., San Diego, CA), and paired-end (2 × 100 base pair) sequencing was performed.

A

B

C
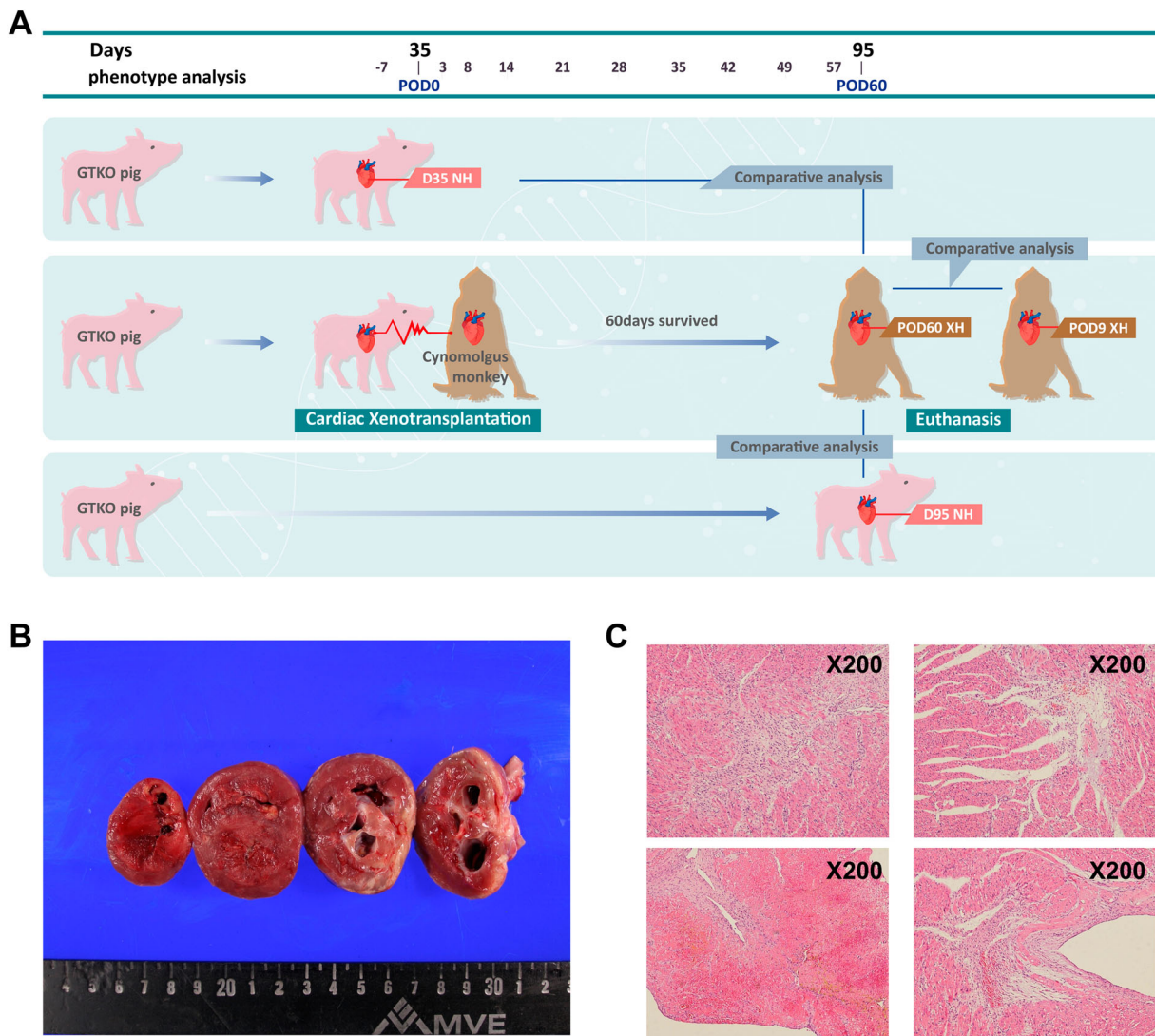
Figure 1. Schematic of experimental design and histological observations for pig-to-monkey cardiac xenotransplantation. (A) Summary of experiments and comparative analyses with time points. Xenotransplantation was performed using the heterotopic abdominal method. Heart samples from a xenotransplanted cynomolgus monkey (POD60 XH) and two age-matched pigs (D35 and D95 NHs) were used in this experiment. Comparison analyses using the previous POD9 XH results were conducted to detect differential gene expression patterns depending on the survival period (Park et al. 2021). (B) XH interior views. The porcine heart weighed 80.62 g at POD60. Cardiac cross-section showed that the atrium space narrowed as the graft thickened. (C) XH photomicrographs showing no evidence of acute cellular and antibody-mediated rejections. Patchy interstitial fibrosis in the myocardium fatty metaplasia in the epicardium and organizing thrombi in the endocardium was observed.

Differentially expressed gene (DEG) and functional analyses

After quality check, trimming, mapping, and counting, raw counts were obtained. DEG analyses were done for POD60 XH as a case versus (vs) D35 and D95 NH as controls. Multidimensional scaling (MDS) was carried out to demonstrate sample similarities. More detailed methods are described in the Supplementary materials and a previous study (Lim et al. 2020). The overlapping DEGs for POD60 XH based on D35 and D95 NH were classified as up- and down-regulated DEGs, and used for functional annotations. Enrichment analyses were performed

with biological processes (BPs) of gene ontology (GO) and pathways of Kyoto Encyclopedia of Genes and Genomes (KEGG) database.

Comparative analyses

Gene-annotated DEGs for POD60 XH were compared with annotated DEGs for POD9 XH based on D31 NH (D9 survived monkey) in our previous study (Park et al. 2021). The DEGs were classified into three types: POD9-specific DEGs, overlapping DEGs, and POD60-specific DEGs, and functional annotations to KEGG

pathways were performed. Network analysis was performed to cluster the enriched KEGG pathways, and we focused on the clustered KEGG pathways having similar molecular functions for functional profiling between POD9 and POD60 monkeys.

Quantitative real-time PCR (qPCR) analyses

To technically validate gene expression in POD60 and POD9, immune-related genes were selected based on FC values, and qPCR was performed using NH and XH samples. Total RNA was extracted from the tissues, and then cDNA was synthesized. The qPCR analyses were performed using StepOne Real-Time PCR system (ABI, Foster City, CA) with SYBR Green. Pig primers used for qPCR are summarized in Table S2.

Results

Recipient blood analyses

Table 1 presents values obtained from the hematological and biochemical analyses. High-sensitivity C-reactive protein (hs-CRP) levels increased immediately after cardiac xenotransplantation in a long-term survived monkey. As hemoglobin (Hb) and hematocrit (Hct) increased rapidly in POD57, aspartate aminotransferase (AST) and alanine aminotransferase (ALT) increased, and antithrombin III (AT III) and protein C decreased. Platelets gradually increased till POD8 and decreased, only to rapidly increase at POD57 and decrease at POD60. Segmented neutrophils were maintained higher than normal, and lymphocytes were lower than normal post-xenotransplantation. Eosinophils gradually decreased from POD28. Prothrombin time (PT) remained constant and rapidly extended at POD60. Troponin I, a myocardial damage indicator, increased at POD3, but briefly decreased after that, and then rapidly increased towards POD60. Lactate dehydrogenase (LDH) decreased slightly from POD8, increased at POD35, then showed a decreasing trend before rapidly increasing to POD60. Hematological analysis of short-term survived monkey (POD9 XH) is shown in a previous study (Park et al. 2021). Upon comparing with POD60 XH, hs-CRP showed a significant difference between POD9 XH and POD60 XH. In the case of POD9 XH, hs-CRP rapidly increased at POD1, but decreased immediately, and then rapidly increased at POD7 just before death (Figure S1).

Histological assessment

Histological changes following XH of a dead monkey were observed at POD60 (Figure 1(B,C)). The transplanted porcine heart grew from 35.00 g to 80.62 g at POD60, taking up most of the monkey's abdominal cavity. The heart transplant suture was maintained without any bleeding. Histological analysis of cardiac cross-sections of the POD60 revealed that the atrium space narrowed as the graft thickened. We observed patchy interstitial fibrosis in the myocardium fatty metaplasia in the epicardium. Organizing thrombi in the endocardium was observed with evidence of neither acute cellular nor antibody-mediated rejection.

Transcriptomic data processing and significant DEGs in XH

406 million paired-end sequence reads were generated from D35 NH (3 replicates), D95 NH (4 replicates), and POD60 XH (3 replicates), showing 40.7 million average number of reads (Table S1). 40.1 million reads per sample passed the trimming process and were mapped to pig reference genome 11.1.100 with 88.86% unique (ranging from 83.30 to 90.86%) and 95.06% overall (ranging from 88.52 to 97.05%) mapping rates.

Cardiac transcriptome data showed clear clustering for each group (D35 NH, D95 NH, and POD60 XH) in MDS (Figure 2(A)). DEGs were identified by comparing the gene expression levels in POD60 XH (D95 porcine heart) with those in D35 and D95 NH. The comparison of POD60 XH vs. D35 NH was designed to identify pre- and post-transplantation survival cardiac differences, and POD60 XH vs. D95 NH was to identify NH and XH cardiac differences at the same-age. 1,804 and 1,655 DEGs were identified in POD60 XH vs. D35 NH and POD60 XH vs. D95 NH, respectively (Figure 2(B)). The overlapping 1,148 DEGs (605 up- and 543 down-regulated DEGs) are shown in a Venn diagram (Figure 2(C)), with their gene information in Table S3. We observed that many DEGs between POD60 XH vs. D35 NH (64%) and POD60 XH vs. D95 NH (69%) were overlapped with the same expression tendency.

Functional annotations of DEGs

Functional enrichment based on the GO (Figure 2(D)) and KEGG (Figure 2(E)) databases was conducted using 1148 overlapping DEGs. For the overlapping 605 up-regulated DEGs, the BPs of GO were enriched to 100 terms indicating representative as the 'chemokine-mediated signaling pathway'. For the overlapping 543 down-regulated DEGs, the BPs of GO were enriched to 34 terms indicating representative as the 'immune response'. The most significant representative terms in

Table 1. Hematological and biochemical blood parameters of recipient cynomolgus monkey.

| Type	Post-Operative Day (POD)											
	POD-7	POD0	POD3	POD8	POD14	POD21	POD28	POD35	POD42	POD49	POD57	POD60
Calcium	10.30	11.00	9.20	9.80	9.50	8.60	8.50	9.00	8.70	8.90	8.40	8.20
Phosphorus	3.60	3.40	5.00	4.20	4.60	4.70	4.40	5.20	4.70	4.40	9.40	3.90
BUN	27.00	26.00	22.00	18.00	20.00	21.00	21.00	21.00	26.00	28.00	63.00	79.00
Uric acid	0.40	0.80	0.10	0.80	0.20	0.40	0.10	3.80	0.20	0.50	0.50	0.30
Creatinine	0.97	0.94	0.73	0.70	0.74	0.86	0.68	0.72	0.56	0.42	0.76	0.52
IDMS MDRD GFR	121.80	126.20	169.00	177.30	166.20	139.70	183.00	171.20	228.70	318.60	160.70	249.00
Na	142.00	145.00	143.00	141.00	146.00	146.00	146.00	119.00	145.00	149.00	151.00	168.00
K	5.20	6.50	5.20	6.80	5.10	4.90	4.70	29.10	5.80	5.50	5.30	5.70
Cl	103.00	105.00	104.00	103.00	106.00	107.00	109.00	124.00	102.00	104.00	106.00	131.00
Total CO$_2$ (TCO2)	20.00	25.00	25.00	25.00	16.00	22.00	21.00	28.00	23.00	25.00	23.00	26.00
High-sensitivity C-reactive protein (hs-CRP)	0.16	1.42	7.54	0.25	0.34	2.92	3.61	1.84	1.66	2.53	1.35	0.79
Aspartate aminotransferase (AST)	53.00	132.00	462.00	98.00	42.00	58.00	54.00	382.00	60.00	63.00	413.00	1345.00
Alanine aminotransferase (ALT)	37.00	60.00	309.00	103.00	45.00	27.00	26.00	36.00	53.00	79.00	166.00	279.00
Total protein	7.10	8.40	5.60	7.10	6.50	5.80	4.90	14.10	4.90	5.20	4.80	3.10
Albumin	4.40	4.80	3.10	3.90	4.00	3.40	2.80	6.60	2.80	3.00	3.00	1.80
Total bilirubin (TBIL)	0.30	0.10	0.30	<0.1	0.20	0.30	0.20	0.40	0.30	0.40	2.00	0.70
Alkaline phosphatase (Alk. Phos)	249.00	247.00	251.00	276.00	265.00	222.00	220.00	220.00	226.00	215.00	325.00	508.00
Cholesterol (Chol)	105.00	91.00	104.00	81.00	95.00	73.00	75.00	81.00	92.00	94.00	25.00	20.00
Gamma-glutamyl transferase (GGT)	48.00	46.00	27.00	42.00	56.00	41.00	39.00	38.00	38.00	34.00	47.00	39.00
Tacrolimus	–	–	14.40	9.30	12.60	7.20	7.80	8.80	8.20	9.30	30.40	30.40
White blood cell (WBC)	16.89	6.22	10.62	14.67	18.36	12.35	13.49	12.49	13.18	15.19	3.30	6.76
Red blood cell (RBC)	6.13	5.93	3.93	4.47	5.00	4.70	4.72	5.07	5.41	5.69	7.36	5.34
Hemoglobin (Hb)	14.40	14.10	9.30	10.50	11.80	11.10	10.90	11.50	11.90	12.10	15.70	11.30
Hematocrit (Hct)	46.50	45.50	29.70	35.30	39.50	37.40	37.40	44.10	41.60	41.60	51.70	38.00
Mean corpuscular volume (MCV)	75.90	76.70	75.60	79.00	79.00	79.60	79.20	87.00	76.90	73.10	70.20	71.20
Mean corpuscular hemoglobin (MCH)	23.50	23.80	23.70	23.50	23.60	23.60	23.10	22.70	22.00	21.30	21.30	21.20
Mean corpuscular hemoglobin concentration (MCHC)	31.00	31.00	31.30	29.70	29.90	29.70	29.10	26.10	28.60	29.10	30.40	29.70
Red cell distribution width (RDW)	14.10	14.80	14.70	17.10	16.20	16.30	15.50	24.60	14.60	14.50	17.10	15.20
Platelet	400.00	448.00	545.00	726.00	412.00	331.00	382.00	560.00	492.00	345.00	708.00	198.00
Plateletcrit (PCT)	0.45	0.47	0.62	0.76	0.45	0.40	0.44	–	0.53	0.36	0.75	0.20
Mean platelet volume (MPV)	11.30	10.50	11.30	10.50	10.90	12.00	11.60	–	10.90	10.40	10.70	10.30
Platelet distribution width (PDW)	12.90	11.70	13.00	11.90	12.60	14.20	13.60	–	13.30	13.70	14.40	12.80
Segmented neutrophils (Seg.neut.)	44.90	89.00	71.70	85.90	89.30	89.20	89.30	78.80	90.60	94.10	77.90	89.90
Lymphocyte	48.40	1.60	1.60	4.20	1.80	2.30	3.30	14.70	3.90	1.40	2.10	2.10
Monocyte	4.60	5.50	25.00	7.90	6.90	6.20	6.80	5.80	5.20	4.30	20.00	7.70
Eosinophil	2.00	3.90	1.60	1.90	1.90	2.20	0.50	0.60	0.20	0.10	0.00	0.00
Basophil	0.10	0.00	0.10	0.10	0.10	0.10	0.10	0.10	0.10	0.10	0.00	0.30
Absolute neutrophil count (ANC)	7584.00	5536.00	7615.00	12602.00	16395.00	11016.00	12047.00	9842.00	11941.00	14294.00	2571.00	6077.00
Prothrombin time and international normalized ratio (PT INR)	0.78	0.77	0.81	0.71	0.75	0.83	0.82	0.82	0.80	0.79	0.82	–	1.95
Prothrombin time % (PT %)	150.00	153.00	142.00	179.00	160.00	134.00	136.00	144.00	147.00	136.00	–	41.00
Prothrombin time sec (PT sec)	8.90	8.80	9.20	8.10	8.60	9.50	9.40	9.10	9.00	9.40	–	22.10
Activated partial thromboplastine time (aPTT)	21.00	19.40	20.60	21.10	19.50	21.40	31.70	23.30	23.00	22.40	–	30.00
Fibrinogen	307.00	418.00	615.00	284.00	327.00	349.00	353.00	323.00	310.00	327.00	–	155.00
Antithrombin ⍰ (AT ⍰)	93.00	103.00	74.00	99.00	124.00	101.00	85.00	81.00	75.00	74.00	–	33.00
Protein C	299.00	298.00	269.00	188.00	332.00	281.00	230.00	261.00	239.00	238.00	–	50.00
D-dimer	0.01	0.01	0.03	0.05	0.00	0.02	0.06	0.00	0.02	0.04	–	0.10
Lactate dehydrogenase (LDH)	1076.00	2138.00	3935.00	2172.00	937.00	868.00	1410.00	5376.00	1327.00	1127.00	–	5624.00
Troponin I	0.01	<0.01	16.85	0.85	0.35	3.67	6.33	3.04	3.67	7.44	–	249.63
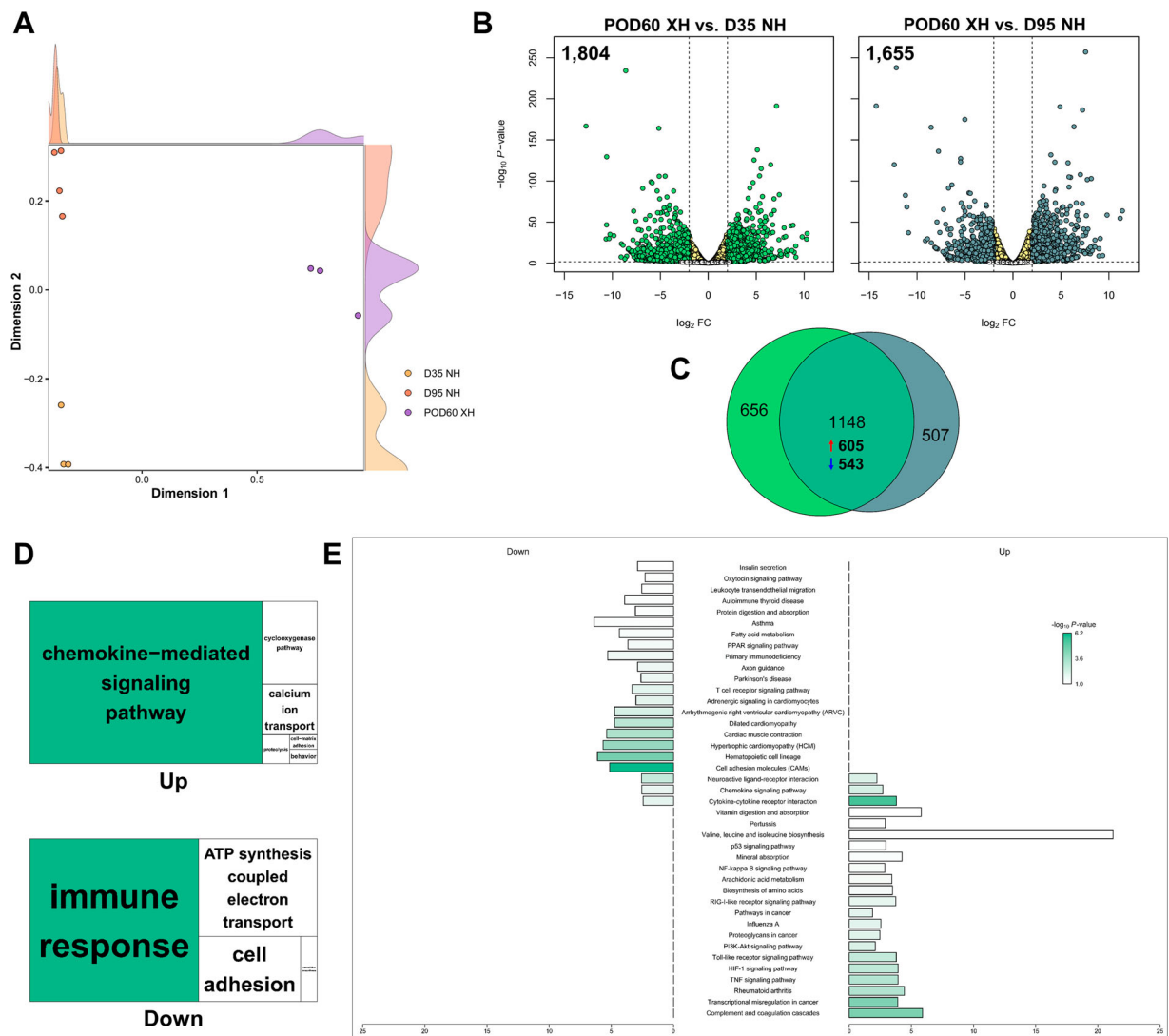
Figure 2. Entire XH transcriptome analyses. (A) Multidimensional scaling showed separate groups among porcine NH and XH transcriptome samples. (B) Volcano plots indicating significant DEGs in XH compared to a normal. (C) Venn diagram described the overlapping number of DEGs between POD60 XH vs. D35 NH and POD60 XH vs. D95 NH. (D) GO treemaps for biological processes were created by overlapping up- and down-regulated DEGs based on the *P*-values. The most significant representative terms were colored green. (E) Pyramid plot indicated KEGG-enriched pathways generated by overlapping up- and down-regulated DEGs with −log10 *P*-values > 1.0.

overlapping up- and down-regulated DEGs were the 'chemokine-mediated signaling pathway' (−log$_{10}$ *P*-value = 7.02) and the 'immune response' (−log$_{10}$ *P*-value = 2.13). Table S4 shows detailed GO enrichment information.

The KEGG enrichment based on the overlapping 605 up-regulated DEGs showed immune signaling-related pathways and cell signaling-related pathways. The KEGG enrichment based on the overlapping 543 down-regulated DEGs showed heart failure-related pathways and fat metabolism-related pathways. Three pathways were identified in both analyses based on up- and down-regulated DEGs. Table S5 shows detailed KEGG enrichment information.

Comparing XHs of long- and short-term survived monkeys

The overlapping 1,148 DEGs for long-term survived monkey (POD60) were gene-annotated to compare with the 1,348 DEGs for short-term survived monkey (POD9) in the previous study (Park et al. 2021), resulting in 824 gene symbols (DEGs for POD60 monkey). Venn diagram showed POD9-specific 988 DEGs, overlapping 360 DEGs, and POD60-specific 464 DEGs (Figure 3(A)).

Functional enrichment based on KEGG pathways is shown in Figure 3(B), and their gene-sharing-based pathway network indicates clusters (Figure 3(C)). The cytokine signaling cluster was significantly common in
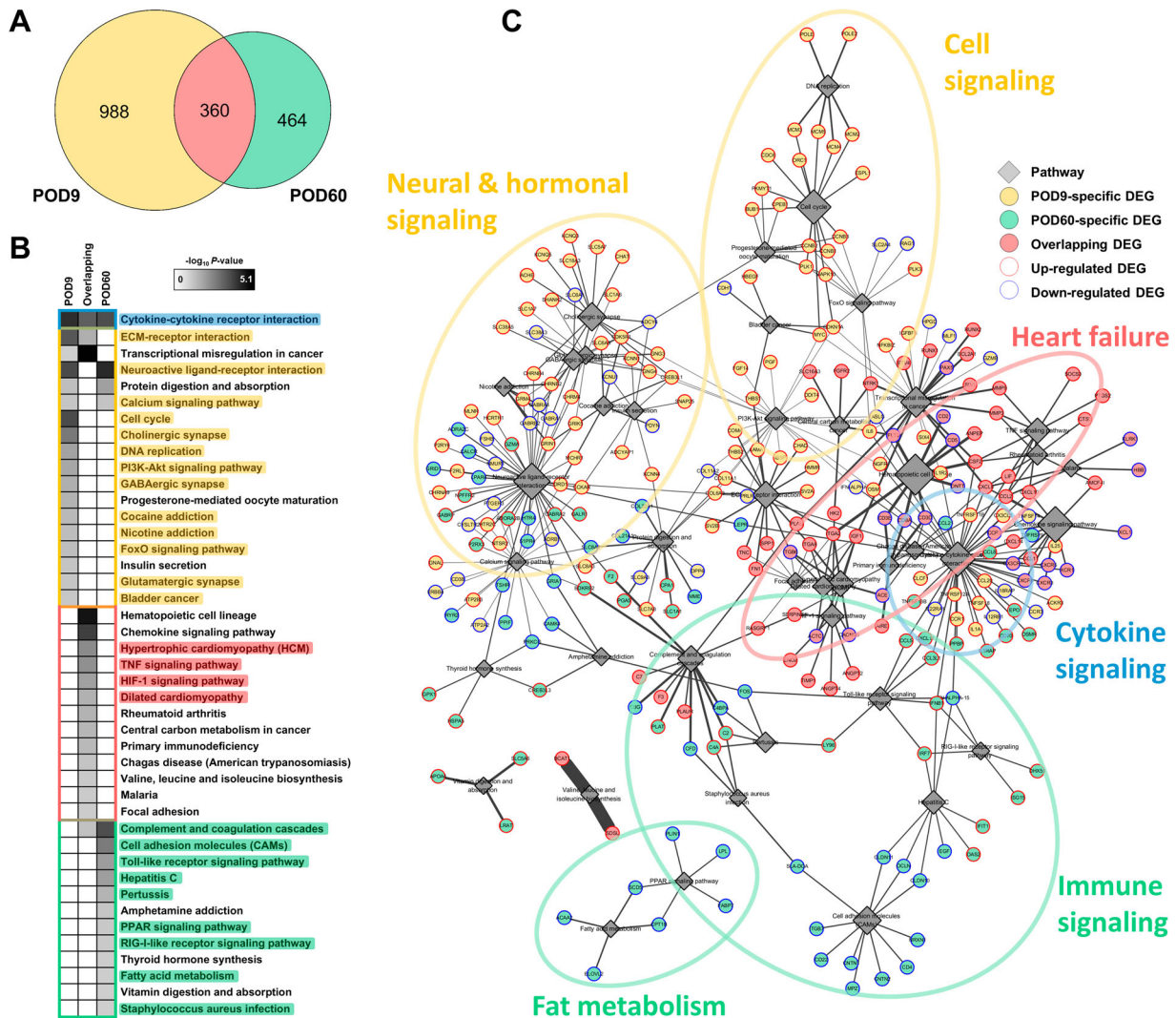
Figure 3. Comparative analyses between POD9 and POD60 cynomolgus monkeys with XH. (A) Venn diagram showing the overlapping DEGs of POD9 and POD60 monkeys with XH. The number of DEGs were indicated after gene annotation. (B) KEGG pathways were enriched using POD9-specific DEGs, overlapping DEGs, and POD60-specific DEGs. Pathways were squared based on functions with colors (cytokine signaling (blue), neural and cell signaling (yellow), heart failure (red), immune signaling and fat metabolism (green)). (C) Functional network based on significantly enriched KEGG pathways. Diamond size indicates significance ($-\log_{10}$ P-value) and line width shows fold enrichment in each pathway. Diamond size for common pathways were calculated as average.

POD9-specific, overlapping, and POD60-specific DEGs. The cell signaling cluster and neural & hormonal signaling significantly showed in POD9-specific DEGs. The heart failure cluster significantly showed in the overlapping DEGs. The immune signaling cluster and fat metabolism significantly showed in POD60-specific DEGs. Interestingly, two neural & hormonal signaling were identified in both POD9 and POD60.

signaling showed 22 POD9-specific, 13 overlapping, and 15 POD60-specific DEGs (proteins) (Figure 4). The 'neuroactive ligand–receptor interaction' gene modulation in neural & hormonal signaling indicated 25 POD9-specific and 18 POD60-specific DEGs (proteins) (Figure S2). The 'cell cycle' gene modulation in cell signaling showed 15 POD9-specific DEGs (proteins) (Figure 5). The 'hypertrophic cardiomyopathy' gene modulation in heart failure showed 7 overlapping DEGs (proteins) (Figure 6).

Gene modulations associated with xenograft survival

We focused on the highly significant pathways for xenograft survival-associated gene modulation. The 'cytokine-cytokine receptor interaction' gene modulation in cytokine

qPCR validations

We performed qPCR experiments using 8 immune-related genes (*IL1A*, *LY96*, *IRF7*, *CCL21*, *FOS*, *CXCR6*, *EGF*, and *IL1RAP*), and identified consistent results with RNA-
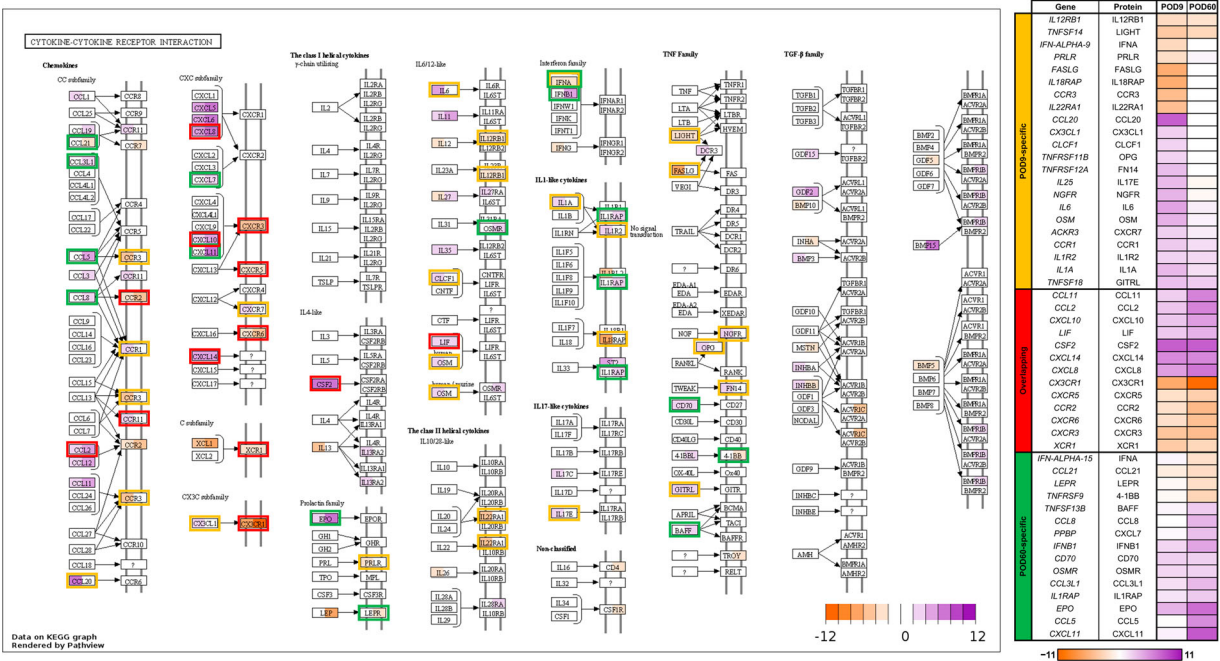
Figure 4. 'Cytokine-cytokine receptor interaction' gene modulation in cytokine signaling associated with xenograft survival. Left and right of proteins show log$_2$ FC of DEGs for POD9 and POD60 monkeys, respectively. Proteins corresponding to DEGs are indicated with a thick border: POD9-specific DEGs (yellow), overlapping DEGs (red), and POD60-specific DEGs (green). The maximum changes (absolute log$_2$ FC) among genes were applied in each protein as the representative values. Heatmap shows gene names corresponding to each protein with log$_2$ FC values of POD9 and POD60 monkeys.
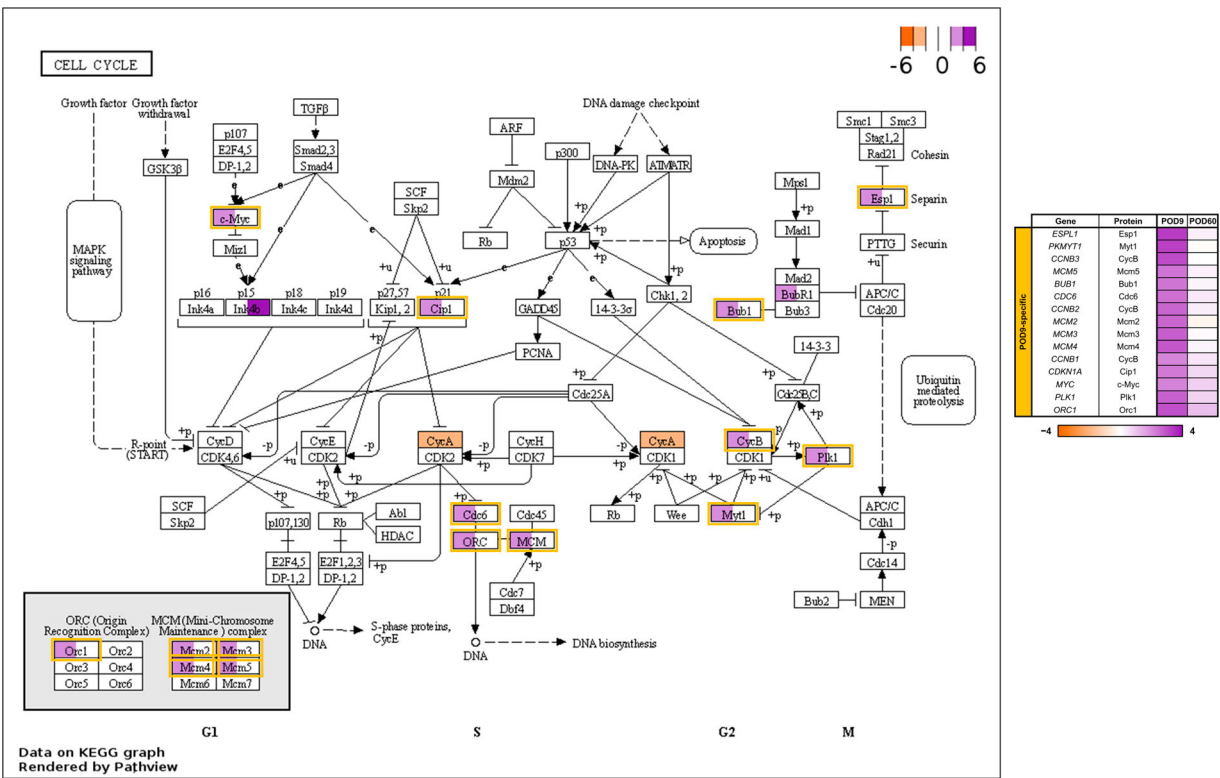
Figure 5. 'Cell cycle' gene modulation in cell signaling associated with xenograft survival. Left and right of proteins show log$_2$ FC of DEGs for POD9 and POD60 monkeys, respectively. Proteins corresponding to DEGs are indicated with a thick border: POD9-specific DEGs (yellow). The maximum changes (absolute log$_2$ FC) among genes were applied in each protein as the representative values. Heatmap shows gene names corresponding to each protein with log$_2$ FC values of POD9 and POD60 monkeys.
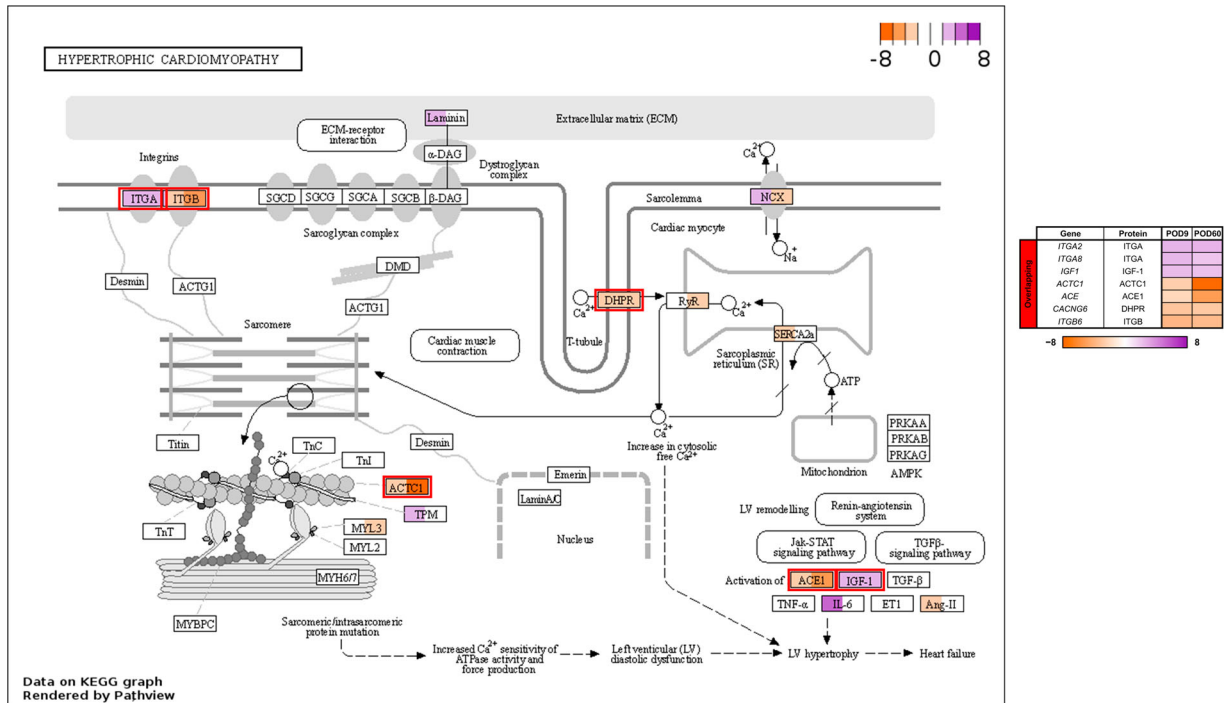
Figure 6. 'Hypertrophic cardiomyopathy' gene modulation in xenograft survival-associated heart failure. Left and right of proteins show log$_2$ FC of DEGs for POD9 and POD60 monkeys, respectively. Proteins corresponding to DEGs are indicated with a thick border: overlapping DEGs (red). The maximum changes (absolute log$_2$ FC) among genes were applied in each protein as the representative values. Heatmap shows gene names corresponding to each protein with log$_2$ FC values of POD9 and POD60 monkeys.

seq except for *IL1A* in POD60 and *CCL21* in POD9 showing different expression tendency (Figure 7). Gene expression was generally very low in the monkey tissues, but *CXCR6* and *EGF* genes were expressed at a relatively high level. This result may suggest high similarity between monkeys and pigs.

Discussion

Gradual heart failure in POD60 cynomolgus monkey

The incidence of HAR and AHXR was greatly reduced in XH of cynomolgus monkeys, therefore their survival periods were extended. Here, we investigated hematological and biochemical features (Table 1) in XH of the longest-survived monkey (POD60) without HAR and AHXR, using GTKO/CD46 pig as a donor (Lee et al. 2018). As a major change during survival, troponin I level increased post-operation at POD3, and then decreased as a recovery. However, it increased from POD21, indicating continuous heart damage till POD60. The monkey endured relatively well, but it rapidly deteriorated from POD49 with heart failure. In addition, we observed increased Hb and Hct levels at POD57, considerably by edema and hemoconcentration due to poor heart function, and increased AST and ALT

levels indicating liver damage. Moreover, albumin and blood coagulation factors (fibrinogen, AT III, and protein C) were decreased, and PT sec was increased at POD60, indicating liver failure. Additionally, dehydration coupled with terminal hemolysis (high BUN, Hb up and falling, Hct up and falling, rising K, rising LDH, falling platelet at late POD, and normal creatinine level) and malnutrition (low albumin at late POD) were observed. Finally, high LDH levels indicated the possibility of multi-organ failure including heart and lung. A similar tendency of phenotypes for heart and lung failure was identified in cardiac xenograft using baboons (Längin et al. 2018). The gene expression associated with phenotypes were shown in Table S6. *LDHA* (LDH) was highly up-regulated (3.39 and 2.80) and *TNNI1* (Troponin I) was down-regulated (−7.28 and −5.47) in both comparisons. Among them, highly regulated *LDHA* expression was consistent with blood phenotype LDH (Table 1).

Transcriptomes and its molecular functions of POD60 XH compared to NHs

We identified functional features based on transcriptomes by comparing POD60 XH of the longest survived monkey and two age-matched NHs. MDS showed three

Figure 7. qPCR validation of gene expression based on RNA-seq results. Pig primers were utilized, and eight genes (*IL1A*, *LY96*, *IRF7*, *CCL21*, *FOS*, 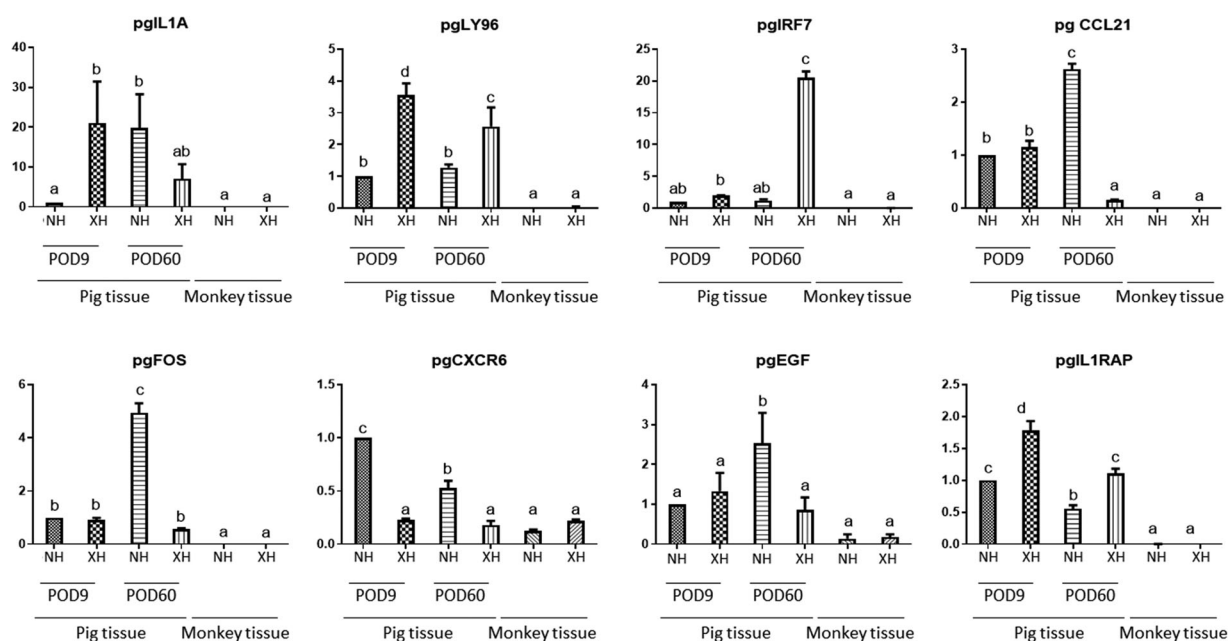*CXCR6*, *EGF*, and *IL1RAP*) were tested. Different lowercase letters above dots show significant differences (*P*-value < 0.0001) among samples as determined by one-way ANOVA with Tukey's multiple comparison test.

distinctly divided clusters for each group using whole transcriptomes (Figure 2(A)). 1,804 and 1,655 DEGs were identified in POD60 XH vs. D35 NH and POD60 XH vs. D95 NH, indicating major transcriptomic changes by xenotransplantation even with strict criteria (FDR < 0.05 and log$_2$ FC ≥ 2) (Figure 2(B)). To reduce age-dependent bias, overlapping 1,148 DEGs (605 up-regulated and 543 down-regulated) were used for functional enrichment analyses (Figure 2(C)), showing significant terms related to immune signaling, neural & hormonal signaling, and heart failure (Figure 2(E)). In xenotransplantation research, pro-inflammatory cytokines are important rejection and coagulopathy features (Ezzelarab et al. 2015; Zhao et al. 2019).

Inflammatory and coagulation-related cytokines (IFNG, TNF-α, IL12, MCP-1, IL8, and IL6) were measured post-transplantation in the serum of pig-to-baboon XH recipients, reporting an increase of MCP-1 and IL6 with a high CRP (Ezzelarab et al. 2015). However, we identified that the expression of *CCL2* (CCL2; MCP-1) and *CXCL8* (CXCL8; IL8) among them was significantly up-regulated in POD60 XH (Table S3). *IL6* expression was not significantly changed post-transplantation in our study: relatively low hs-CRP level was postulated (Table 1), but CC and presumably TM were observed (Figure 1(B)). Pro-inflammatory chemokine CXCL8 recruits and activates neutrophils during inflammation (French et al. 2018). It is believed that the CXCL8 was up-regulated in XH, not serum, due to CXCL8-mediated chemotaxis. We also confirmed that immune-related genes (*CD2*,

CD4, *CD6*, *CD8A*, *CD22*, *CD226,* and *SLA-DOA*) were significantly down-regulated in POD60 XH (Table S3). CD4 and CD8, coreceptors for T cell receptors, assist in communicating with antigen-presenting cells (APCs) having major histocompatibility complex (MHC) class II and I, respectively. Reportedly, CD2, CD6, and CD226 were expressed in T cells (Sayre and Reinherz 1988; Bowen et al. 1995; Bottino et al. 2003), and CD22 in B cells (Crocker et al. 1998). These results suggest that XH T and B cells were mainly suppressed and rejection-protected by immunosuppressive therapies.

We also identified that *ACTC1*, *ACE*, and *CACNG6* were down-regulated, while *IGF1* was up-regulated in POD60 XH (Table S3). *ACTC1* in skeletal muscle affects muscle contraction related to pump function and causes heart failure with reduced expression (Jiang et al. 2010). In addition, ACE inhibition dilates the blood vessels and lowers pressure, resulting in reduced heart failure (Flather et al. 2000). Moreover, abnormal Ca^{2+} handling is a key yet unclear pathophysiological mechanism in heart failure (Lou et al. 2012), which might consider the down-regulated calcium channel stabilizer *CACNG6*. Furthermore, high circulating IGF1 levels are reportedly associated with heart failure, including hypertrophy (Al-Obaidi et al. 2001). Therefore, cardiac xenotransplantation indicates comparable transcriptomic features of heart failure except for the *ACE* gene.

Changes in the nervous system and hormone signaling changes have been reported to be involved in heart failure (Lymperopoulos et al. 2013; Oakley et al. 2013). In

this study, adrenergic receptor-related *ADRA2C* was significantly down-regulated in POD60 XH, but cholinergic receptor genes were not changed (Table S3). In addition, thyroid stimulating and calcitonin hormone receptor genes, *TSHR* and *CALCR* were significantly down-regulated (Table S3). *TSHR* was reported to induce B-type natriuretic peptide, suggesting a role in heart failure-associated hypothyroidism (Huang et al. 2014), while *CALCR* plays a critical role in calcium homeostasis, thereby affecting heart function (Maïmoun and Sultan 2009). These results indicate that heart failure occurred due to abnormal neural activities and multi-organ failure influenced by dysregulated hormonal signaling. Taken all together, we show that long-term survived cynomolgus XH exhibits specific transcriptomic differences in immune, neural, and hormonal signaling pathways, which may play crucial roles in heart failure.

Transcriptomic differences of heart failure between long- and short-term survived monkeys

The 1,348 annotated genes of POD60 XH in this study were compared with the 824 ones of POD9 XH in a previous study (Figure 3(A)) (Park et al. 2021). Among them, 360 overlapping genes were significantly enriched (Figure 3(B)) and clustered (Figure 3(C)); we focused on 'hypertrophic cardiomyopathy' to identify gene modulations in heart failure (Figure 6). *ITGA2*, *ITGA8*, and *IGF1* were commonly up-regulated in POD60 and POD9 XHs, while *ACTC1*, *ACE*, *CACNG6*, and *ITGB6* were commonly down-regulated. Transcriptomic changes of down-regulated *ACTC1*, *ACE*, *CACNG6*, and up-regulated *IGF1*, indicate similar heart failure signatures between POD60 and POD9 (Flather et al. 2000; Al-Obaidi et al. 2001; Jiang et al. 2010; Lou et al. 2012). However, only POD9 XH showed significantly up-regulated *IL6*, which participates in the innate immune response. IL6 induces acute-phase proteins, CRP, complement system proteins, and a coagulation cascade (Villar-Fincheira et al. 2021), which can result in coagulopathy. In fact, POD60 XH showed a relatively low hs-CRP level (Figure 7), but CC and presumably TM were present (Figure 1(B)) similar to POD9 XH (Park et al. 2021). Therefore, both long- and short-term survived monkeys have comparable transcriptomic features for heart failure except cytokine signaling.

Up-regulated cell signaling in short-term survived monkey

Heart remodeling occurs post-transplantation, and heart failure ensues if the remodeling lasts (Raichlin et al. 2009). A previous study also suggests that residual cardiomyocytes in impaired hearts re-enter the cell cycle to obtain proliferative capacity by cell cycle-related gene alterations or growth-related signal regulation (Azevedo et al. 2015). In our study, significant cell signaling-related pathways were identified by enrichment analysis using POD9-specific 988 DEGs (Figure 3). We focused on the 'cell cycle' term to identify gene modulations in cell signaling (Figure 5). Fifteen genes (*MYC*, *CDKN1A*, *CDC6*, *ORC1*, *MCM2*, *MCM3*, *MCM4*, *MCM5*, *BUB1*, *CCNB1*, *CCNB2*, *CCNB3*, *PKMYT1*, *PLK1*, and *ESPL1*) were up-regulated in POD9 XH, but not in POD60 XH. *MYC* plays an important role in regulating cell growth, apoptosis, and differentiation (Dang 1999). *CDKN1A* encoded p21, which induces p53-dependent cell cycle arrest in response to DNA damage (Engeland 2018). *CDC6* plays an important role in cell cycle coordination of the S phase (Borlado and Méndez 2008). *ORC1* encodes highly conserved six subunits protein complex essential for DNA replication initiation (Hossain et al. 2021). In addition, *MCM2*, *MCM3*, *MCM4*, and *MCM5* also encode highly conserved mini-chromosome maintenance proteins for genome replication initiation (Maiorano et al. 2006). Moreover, *BUB1* was reported to affect spindle assembly checkpoint and chromosome alignment during metaphase (Meraldi and Sorger 2005), and *CCNB1*, *CCNB2*, and *CCNB3* were known to encode mitosis regulatory proteins for G2/M transition phase control (Wu et al. 2010; Farshadi et al. 2019). *PKMYT1* encoded Myt1, which inactivates cell cycle Cdks through phosphorylation (Booher et al. 1997). *PLK1* encoded plk1, which supports centrosome maturation in late G2/early prophase and the bipolar spindle establishment (Alfaro et al. 2021). *ESPL1* regulates the sister chromatid separation (Guo et al. 2013). In summary, we found several critical genes up-regulated in POD9 XH and hypothesize that heart remodeling and regeneration are induced. Consequently, it is believed that heart remodeling and regeneration can further adversely affect XH and its survival period.

Differences in neural and hormonal signaling

Unbalanced neural and hormonal signaling can lead to heart failure (Lymperopoulos et al. 2013; Oakley et al. 2013). We identified significant pathways related to neural and hormonal signaling (Figure 3) and focused on the 'neuroactive ligand–receptor interaction' term to find out specific gene modulations (Figure S2). Remarkably, adrenergic-related *ADRA2C* was down-regulated only in POD60 XH for this study, while cholinergic-related *CHRM4*, *CHRNB2*, and *CHRNB4* were up-regulated only in POD9 XH. *ADRA2C* was reported to have a critical role in regulating neurotransmitter

release from sympathetic nerves and adrenergic neurons (Bücheler et al. 2002). *CHRM4*, *CHRNB2*, and *CHRNB4* were known to regulate cellular responses, including ion channel mediation by binding acetylcholine (Resende and Adhikari 2009). In addition, *TSHR* and *CALCR* encoding hormone receptors were down-regulated only in POD60 XH, indicating an unbalancing expression of receptors that can lead to multi-organ failure, especially thyroid (Klein and Ojamaa 2001). In the POD60 XH, high LDH indicated multi-organ failure risk (Table 1). To sum up, we confirm and suggest that multi-organ failure by unbalanced expression of receptors in neural and hormonal signaling is associated with long-term XH survival.

Immunological differences based on transcriptomes

Immunosuppression is important to avoid immune rejection in xenotransplantation. Recently, HAR and AHXR in the early xenograft period were dramatically reduced by using GTKO pigs (Mohiuddin et al. 2014, 2016). Cellular xenograft rejection may occur days to weeks post-transplantation and is mediated by innate and adaptive immune responses (Cadili and Kneteman 2008). In this study, we identified significant immune signaling-related pathways (Figure 3) and focused on the 'cell adhesion molecules' term to identify gene modulations (Figure S3). *CD4*, *CD22*, and *SLA-DOA* were significantly down-regulated only in POD60 XH. CD4 assists in communicating with APCs such as B cells using MHC class II, inducing maturation of helper T cells for both innate and adaptive immune responses. In addition, CD22 plays a key role in B cell responses and innate immunity (Clark and Giltiay 2018). *CD2*, *CD6*, *CD8A*, and *CD226* were commonly down-regulated in both POD60 and POD9. CD2, CD6, and CD226 play a critical role in T cell activation (Carrasco et al. 2017; Binder et al. 2020; Huang et al. 2020). CD8 recognizes APCs expressing MHC class I, and the interaction induces maturation of cytotoxic T cells (O'Rourke and Mescher 1993). Collectively, T cell activation was commonly suppressed in both long- and short-term survived monkeys, but B cell activation was more suppressed in long-term survived monkey. Besides immunosuppression, cytokine signaling changes were also identified (Figure 3), and we focused on highly regulated genes. *CX3CR1* was commonly down-regulated in POD60 and POD9 XHs (Figure 4). CX3CR1 is involved in leukocyte adhesion, and it is reported that inhibiting CX3CR1 significantly prolonged mouse cardiac allograft survival (Robinson et al. 2000). We confirmed that *CX3CR1* was more down-regulated in POD60 than in POD9, resulting

in relatively long-term survival in POD60. CCL20, CCL5, and CXCL11 play an important role in the attraction of leukocytes. *CCL20* was up-regulated in POD9, while *CCL5* and *CXCL11* were up-regulated in POD60. *CCL5*-encoded RANTES is a pivotal mediator of the cellular infiltrate in graft atherosclerosis (Pattison et al. 1996) and is important for macrophage recruitment in cardiac allograft rejection (Azzawi et al. 1998). Additionally, POD9 showed significantly up-regulated proinflammatory cytokines *IL1a* and *IL6*, which can mediate toxic effects by promoting macrophages (El-Ouaghlidi et al. 1999). Therefore, both long- and short-term survived monkey XHs indicate transcriptome-regulated chemotaxis features of leukocytes including macrophages, and proinflammatory cytokines may play a major role in determining the survival period.

Conclusions

We performed pig-to-cynomolgus monkey cardiac xenotransplantation using GTKO/CD46 pigs. Hematological, biochemical, and histological analyses were conducted on the xenotransplanted monkey. In addition to phenotypic measurement, RNA-seq-based transcriptomes were produced in POD60 XH and age-matched NHs. DEG profiling in POD60 XH compared to NHs was performed, and its functions were identified. We compared POD60 with POD9 using annotated genes to identify long- and short-term survival differences. In the functional network, 6 clusters (cytokine signaling, cell signaling, neural & hormonal signaling, heart failure, immune signaling, and fat metabolism) were identified. Heart failures were shown in both long- and short-term survived XHs. However, heart remodeling and regeneration signaling was up-regulated only in short-term survived XH. Moreover, heart failure and multi-organ failure features by neural and hormonal signaling in long-term survived XH were confirmed. In terms of immune signaling, T cell activation was inhibited in both, but only long-term survived XH showed B cell suppression. In addition, rejection-inducing chemotaxis features were identified and proinflammatory cytokines were confirmed only in short-term survived XH. These results provide the first discovery of differential heart failure development by survival periods at the transcriptome level and suggest candidate genes in each signaling to control side effects in heart xenotransplantation.

Disclosure statement

ORCID

Byeonghwi Lim ⓘ http://orcid.org/0000-0001-8489-0044
Min-Jae Jang ⓘ http://orcid.org/0000-0001-7404-4258
Seung-Mi Oh ⓘ http://orcid.org/0000-0001-9634-2280
Jin Gu No ⓘ http://orcid.org/0000-0002-7851-7662
Jungjae Lee ⓘ http://orcid.org/0000-0002-6145-8862
Sang Eun Kim ⓘ http://orcid.org/0000-0002-8282-6898
Sun A. Ock ⓘ http://orcid.org/0000-0002-0887-8200
Ik Jin Yun ⓘ http://orcid.org/0000-0003-4013-6714
Junseok Kim ⓘ http://orcid.org/0000-0002-2547-9674
Hyun Keun Chee ⓘ http://orcid.org/0000-0001-7041-352X
Wan Seop Kim ⓘ http://orcid.org/0000-0001-7704-5942
Hee Jung Kang ⓘ http://orcid.org/0000-0003-1249-6181
Kahee Cho ⓘ http://orcid.org/0000-0001-7554-9282
Keon Bong Oh ⓘ http://orcid.org/0000-0002-0651-0306
Jun-Mo Kim ⓘ http://orcid.org/0000-0002-6934-398X

References

Ahn JS, Won J-H, Kim D-Y, Jung S-E, Kim B-J, Kim J-M, Ryu B-Y. 2022. Transcriptome alterations in spermatogonial stem cells exposed to bisphenol A. Animal Cells Syst. 26(2):70–83. doi:10.1080/19768354.2022.2061592.

Alfaro E, López-Jiménez P, González-Martínez J, Malumbres M, Suja JA, Gómez R. 2021. PLK1 regulates centrosome migration and spindle dynamics in male mouse meiosis. EMBO Rep. 22(4):e51030. doi:10.15252/embr.202051030.

Al-Obaidi M, Hon J, Stubbs P, Barnes J, Amersey R, Dahdal M, Laycock J, Noble M, Alaghband-Zadeh J. 2001. Plasma insulin-like growth factor-1 elevated in mild-to-moderate but not severe heart failure. Am Heart J. 142(6):11A–15A. doi:10.1067/mhj.2001.118116.

Azevedo PS, Polegato BF, Minicucci MF, Paiva SA, Zornoff LA. 2015. Cardiac remodeling: concepts, clinical impact, pathophysiological mechanisms and pharmacologic treatment. Arq Bras Cardiol. 106:62–69.

Azzawi M, Hasleton P, Geraghty P, Yonan N, Krysiak P, El-Gammal A, Deiraniya A, Hutchinson I. 1998. RANTES chemokine expression is related to acute cardiac cellular rejection and infiltration by CD45RO T-lymphocytes and macrophages. J Heart Lung Transpl. 17(9):881–887.

Binder C, Cvetkovski F, Sellberg F, Berg S, Paternina Visbal H, Sachs DH, Berglund E, Berglund D. 2020. CD2 immunobiology. Front Immunol. 11:1090. doi:10.3389/fimmu.2020.01090.

Booher RN, Holman PS, Fattaey A. 1997. Human Myt1 is a cell cycle-regulated kinase that inhibits Cdc2 but not Cdk2 activity. J Biol Chem. 272(35):22300–22306. doi:10.1074/jbc.272.35.22300.

Borlado LR, Méndez J. 2008. CDC6: from DNA replication to cell cycle checkpoints and oncogenesis. Carcinogenesis. 29(2):237–243. doi:10.1093/carcin/bgm268.

Bottino C, Castriconi R, Pende D, Rivera P, Nanni M, Carnemolla B, Cantoni C, Grassi J, Marcenaro S, Reymond N. 2003. Identification of PVR (CD155) and Nectin-2 (CD112) as cell surface ligands for the human DNAM-1 (CD226) activating molecule. J Exp Med. 198(4):557–567. doi:10.1084/jem.20030788.

Bowen MA, Patel DD, Li X, Modrell B, Malacko AR, Wang W-C, Marquardt H, Neubauer M, Pesando JM, Francke U. 1995. Cloning, mapping, and characterization of activated leukocyte-cell adhesion molecule (ALCAM), a CD6 ligand. J Exp Med. 181(6):2213–2220. doi:10.1084/jem.181.6.2213.

Bücheler MM, Hadamek K, Hein L. 2002. Two α2-adrenergic receptor subtypes, α2A and α2C, inhibit transmitter release in the brain of gene-targeted mice. Neuroscience. 109(4):819–826. doi:10.1016/S0306-4522(01)00531-0.

Bühler L, Basker M, Alwayn I, Goepfert C, Kitamura H, Kawai T, Gojo S, Kozlowski T, Ierino F, Awwad M. 2000. Coagulation and thrombotic disorders associated with pig organ and hematopoietic cell transplantation in nonhuman primates. Transplantation. 70(9):1323–1331. doi:10.1097/00007890-200011150-00010.

Cadili A, Kneteman N. 2008. The role of macrophages in xenograft rejection. Transplant Proc. 40(10):3289–3293. doi:10.1016/j.transproceed.2008.08.125.

Carrasco E, Escoda-Ferran C, Climent N, Miró-Julià C, Simões IT, Martínez-Florensa M, Sarukhan A, Carreras E, Lozano F. 2017. Human CD6 down-modulation following T-cell activation compromises lymphocyte survival and proliferative responses. Front Immunol. 8:769. doi:10.3389/fimmu.2017.00769.

Cascalho M, Platt JL. 2001. Xenotransplantation and other means of organ replacement. Nat Rev Immunol. 1(2):154–160. doi:10.1038/35100578.

Clark EA, Giltiay NV. 2018. CD22: a regulator of innate and adaptive B cell responses and autoimmunity. Front Immunol. 9(1):2235. doi:10.3389/fimmu.2018.02235.

Cooper DK, Bottino R. 2015. Recent advances in understanding xenotransplantation: implications for the clinic. Expert Rev Clin Immunol. 11(12):1379–1390. doi:10.1586/1744666X.2015.1083861.

Cooper DK, Ezzelarab MB, Hara H, Iwase H, Lee W, Wijkstrom M, Bottino R. 2016. The pathobiology of pig-to-primate xenotransplantation: a historical review. Xenotransplantation. 23(2):83–105. doi:10.1111/xen.12219.

Cooper DK, Gollackner B, Sachs DH. 2002. Will the pig solve the transplantation backlog? Annu Rev Med. 53(1):133–147. doi:10.1146/annurev.med.53.082901.103900.

Cooper DK, Pierson RN. 2022. The future of cardiac xenotransplantation. Nat Rev Cardiol. 19(5):281–282.

Cooper DK, Satyananda V, Ekser B, van der Windt DJ, Hara H, Ezzelarab MB, Schuurman HJ. 2014. Progress in pig-to-nonhuman primate transplantation models (1998–2013): a comprehensive review of the literature. Xenotransplantation. 21(5):397–419. doi:10.1111/xen.12127.

Crocker PR, Clark E, Filbin M, Gordon S, Jones Y, Kehrl J, Kelm S, Le Douarin N, Powell L, Roder J. 1998. Siglecs: a family of sialic-acid binding lectins. Glycobiology. 8(2):v–vi.

Dang CV. 1999. c-Myc target genes involved in cell growth, apoptosis, and metabolism. Mol Cell Biol. 19(1):1–11. doi:10.1128/MCB.19.1.1.

El-Ouaghlidi A, Jahr H, Pfeiffer G, Hering B, Brandhorst D, Brandhorst H, Federlin K, Bretzel R. 1999. Cytokine mRNA expression in peripheral blood cells of immunosuppressed human islet transplant recipients. J Mol Med. 77(1):115–117. doi:10.1007/s001090050315.

Engeland K. 2018. Cell cycle arrest through indirect transcriptional repression by p53: I have a DREAM. Cell Death Differ. 25(1):114–132. doi:10.1038/cdd.2017.172.

Ezzelarab MB, Ekser B, Azimzadeh A, Lin CC, Zhao Y, Rodriguez R, Echeverri GJ, Iwase H, Long C, Hara H. 2015. Systemic inflammation in xenograft recipients precedes activation of coagulation. Xenotransplantation. 22(1):32–47. doi:10.1111/xen.12133.

Farshadi E, Yan J, Leclere P, Goldbeter A, Chaves I, van der Horst GT. 2019. The positive circadian regulators CLOCK and BMAL1 control G2/M cell cycle transition through Cyclin B1. Cell Cycle. 18(1):16–33. doi:10.1080/15384101.2018.1558638.

Fischer K, Kraner-Scheiber S, Petersen B, Rieblinger B, Buermann A, Flisikowska T, Flisikowski K, Christan S, Edlinger M, Baars W. 2016. Efficient production of multi-modified pigs for xenotransplantation by 'combineering', gene stacking and gene editing. Sci Rep. 6(1):1–11. doi:10.1038/s41598-016-0001-8.

Flather MD, Yusuf S, Køber L, Pfeffer M, Hall A, Murray G, Torp-Pedersen C, Ball S, Pogue J, Moyé L. 2000. Long-term ACE-inhibitor therapy in patients with heart failure or left-ventricular dysfunction: a systematic overview of data from individual patients. Lancet. 355(9215):1575–1581. doi:10.1016/S0140-6736(00)02212-1.

French BM, Sendil S, Sepuru KM, Ranek J, Burdorf L, Harris D, Redding E, Cheng X, Laird CT, Zhao Y. 2018. Interleukin-8 mediates neutrophil-endothelial interactions in pig-to-human xenogeneic models. Xenotransplantation. 25(2):e12385. doi:10.1111/xen.12385.

Guo G, Sun X, Chen C, Wu S, Huang P, Li Z, Dean M, Huang Y, Jia W, Zhou Q. 2013. Whole-genome and whole-exome sequencing of bladder cancer identifies frequent alterations in genes involved in sister chromatid cohesion and segregation. Nat Genet. 45(12):1459–1463. doi:10.1038/ng.2798.

Hossain M, Bhalla K, Stillman B. 2021. Multiple, short protein binding motifs in ORC1 and CDC6 control the initiation of DNA replication. Mol Cell. 81(9):1951–1969. doi:10.1016/j.molcel.2021.03.003.

Huang W, Xu J, Jing F, Chen W-B, Gao L, Yuan H-T, Zhao J-J. 2014. Functional thyrotropin receptor expression in the ventricle and the effects on ventricular BNP secretion. Endocrine. 46(2):328–339. doi:10.1007/s12020-013-0052-6.

Huang Z, Qi G, Miller JS, Zheng SG. 2020. CD226: an emerging role in immunologic diseases. Front Cell Dev Biol. 8:564. doi:10.3389/fcell.2020.00564.

Jiang H-K, Qiu G-R, Li-Ling J, Xin N, Sun K-L. 2010. Reduced ACTC1 expression might play a role in the onset of congenital heart disease by inducing cardiomyocyte apoptosis. Circ J. 74(11):2410–2418. doi:10.1253/circj.CJ-10-0234.

Kim HS, Kim J, Kim J, Choi YH. 2022. Characterization of differential gene expression of broiler chicken to thermal stress in discrete developmental stages. Animal Cells Syst. 26(2):62–69. doi:10.1080/19768354.2022.2059566.

Klein I, Ojamaa K. 2001. Thyroid hormone and the cardiovascular system. N Engl J Med. 344(7):501–509. doi:10.1056/NEJM200102153440707.

Kobashigawa J. 2022. Pig-to-human heart transplantation: culmination of technology and ingenuity. Ann Thorac Surg. 113(3):711. doi:10.1016/j.athoracsur.2022.01.008.

Längin M, Mayr T, Reichart B, Michel S, Buchholz S, Guethoff S, Dashkevich A, Baehr A, Egerer S, Bauer A. 2018. Consistent success in life-supporting porcine cardiac xenotransplantation. Nature. 564(7736):430–433. doi:10.1038/s41586-018-0765-z.

Lee SJ, Kim JS, Chee HK, Yun IJ, Park KS, Yang HS, Park JH. 2018. Seven years of experiences of preclinical experiments of xeno-heart transplantation of pig to non-human primate (Cynomolgus monkey). Transplant Proc. 50(4):1167–1171. doi:10.1016/j.transproceed.2018.01.041.

Lim B, Kim S, Lim K-S, Jeong C-G, Kim S-C, Lee S-M, Park C-K, Te Pas MFW, Gho H, Kim T-H, et al. 2020. Integrated time-serial transcriptome networks reveal common innate and tissue-specific adaptive immune responses to PRRSV infection. Vet Res. 51(1):128. doi:10.1186/s13567-020-00850-5.

Long AT, Kenne E, Jung R, Fuchs TA, Renné T. 2016. Contact system revisited: an interface between inflammation, coagulation, and innate immunity. J Thromb Haemostasis. 14(3):427–437. doi:10.1111/jth.13235.

Lou Q, Janardhan A, Efimov IR. 2012. Remodeling of calcium handling in human heart failure. Calc Signal. 740(1):1145–1174.

Lu T, Yang B, Wang R, Qin C. 2020. Xenotransplantation: current status in preclinical research. Front Immunol. 10:3060. doi:10.3389/fimmu.2019.03060.

Lund LH, Khush KK, Cherikh WS, Goldfarb S, Kucheryavaya AY, Levvey BJ, Meiser B, Rossano JW, Chambers DC, Yusen RD. 2017. The Registry of the International Society for Heart and Lung Transplantation: thirty-fourth adult heart transplantation report—2017; focus theme: allograft ischemic time. J Heart Lung Transplant. 36(10):1037–1046. doi:10.1016/j.healun.2017.07.019.

Lymperopoulos A, Rengo G, Koch WJ. 2013. Adrenergic nervous system in heart failure: pathophysiology and therapy. Circ Res. 113(6):739–753. doi:10.1161/CIRCRESAHA.113.300308.

Maiorano D, Lutzmann M, Méchali M. 2006. MCM proteins and DNA replication. Curr Opin Cell Biol. 18(2):130–136. doi:10.1016/j.ceb.2006.02.006.

Maïmoun L, Sultan C. 2009. Effect of physical activity on calcium homeostasis and calciotropic hormones: a review. Calcif Tissue Int. 85(4):277–286. doi:10.1007/s00223-009-9277-z.

Meraldi P, Sorger PK. 2005. A dual role for Bub1 in the spindle checkpoint and chromosome congression. EMBO J. 24(8):1621–1633. doi:10.1038/sj.emboj.7600641.

Mohiuddin MM, Singh AK, Corcoran PC, Hoyt RF, Thomas ML, Lewis BG, Eckhaus M, Dabkowski NL, Belli AJ, Reimann KA. 2014. Role of anti-CD40 antibody-mediated costimulation blockade on non-Gal antibody production and heterotopic cardiac xenograft survival in a GTKO. hCD46Tg pig-to-baboon model. Xenotransplantation. 21(1):35–45. doi:10.1111/xen.12066.

Mohiuddin MM, Singh AK, Corcoran PC, Thomas ML, Clark T, Lewis BG, Hoyt RF, Eckhaus M, Pierson RN, Belli AJ. 2016. Chimeric 2C10R4 anti-CD40 antibody therapy is critical for long-term survival of GTKO. hCD46. hTBM pig-to-primate cardiac xenograft. Nat Commun. 7(1):1–10. doi:10.1038/ncomms11138.

Oakley RH, Ren R, Cruz-Topete D, Bird GS, Myers PH, Boyle MC, Schneider MD, Willis MS, Cidlowski JA. 2013. Essential role of stress hormone signaling in cardiomyocytes for the prevention of heart disease. Proc Natl Acad Sci USA. 110(42):17035–17040. doi:10.1073/pnas.1302546110.

O'Rourke AM, Mescher MF. 1993. The roles of CD8 in cytotoxic T lymphocyte function. Immunol Today. 14(4):177–183. doi:10.1016/0167-5699(93)90283-Q.

Park MY, Vasamsetti K, Kim BM, Kang WS, Kim HJ, Lim D-Y, Cho B, Kim K, Chee JS, Park HK, H J. 2021. Comprehensive analysis of cardiac xeno-graft unveils rejection mechanisms. Int J Mol Sci. 22(2):751. doi:10.3390/ijms22020751.

Pattison JM, Nelson PJ, Huie P, Sibley RK, Krensky AM. 1996. RANTES chemokine expression in transplant-associated accelerated atherosclerosis. J Heart Lung Transplant. 15 (12):1194–1199.

Raichlin E, Villarraga H, Chandrasekaran K, Clavell A, Frantz R, Kushwaha S, Rodeheffer R, McGregor C, Daly R, Park S. 2009. Cardiac allograft remodeling after heart transplantation is associated with increased graft vasculopathy and mortality. Am J Transpl. 9(1):132–139. doi:10.1111/j.1600-6143.2008.02474.x.

Resende RR, Adhikari A. 2009. Cholinergic receptor pathways involved in apoptosis, cell proliferation and neuronal differentiation. Cell Commun Signal. 7(1):1–20. doi:10.1186/1478-811X-7-20.

Robinson LA, Nataraj C, Thomas DW, Howell DN, Griffiths R, Bautch V, Patel DD, Feng L, Coffman TM. 2000. A role for fractalkine and its receptor (CX3CR1) in cardiac allograft rejection. J Immunol. 165(11):6067–6072. doi:10.4049/jimmunol.165.11.6067.

Rossano JW, Cherikh WS, Chambers DC, Goldfarb S, Khush K, Kucheryavaya AY, Levvey BJ, Lund LH, Meiser B, Yusen RD. 2017. The Registry of the International Society for Heart and Lung Transplantation: twentieth pediatric heart transplantation report—2017; focus theme: allograft ischemic time. J Heart Lung Transplant. 36(10):1060–1069. doi:10.1016/j.healun.2017.07.018.

Sayre P, Reinherz E. 1988. Structure and function of the erythrocyte receptor CD2 on human T lymphocytes: a review. Scand J Rheumatol. 17(Suppl. 76):131–144. doi:10.3109/03009748809102963.

Villar-Fincheira P, Sanhueza-Olivares F, Norambuena-Soto I, Cancino-Arenas N, Hernandez-Vargas F, Troncoso R, Gabrielli L, Chiong M. 2021. Role of interleukin-6 in vascular health and disease. Front Mol Biosci. 8:79. doi:10.3389/fmolb.2021.641734.

Wu T, Zhang X, Huang X, Yang Y, Hua X. 2010. Regulation of cyclin B2 expression and cell cycle G2/m transition by menin. J Biol Chem. 285(24):18291–18300. doi:10.1074/jbc.M110.106575.

Yang HS, Chee HK, Kim JS, Kim WS, Park JH, Shin KC, Park KS, Lee SW, Cho KH, Park WJ. 2017. Non-invasive myocardial strain imaging to evaluate graft failure in cardiac xenotransplantation. J Korean Soc Transpl. 31(1):25–33. doi:10.4285/jkstn.2017.31.1.25.

Zhao Y, Cooper DK, Wang H, Chen P, He C, Cai Z, Mou L, Luan S, Gao H. 2019. Potential pathological role of pro-inflammatory cytokines (IL-6, TNF-α, and IL-17) in xenotransplantation. Xenotransplantation. 26(3):e12502. doi:10.1111/xen.12502.